Supporting Information

Evans *et al.* 10.1073/pnas.0808270106

Materials and Methods

Purification of His_6-Tagged Aryl Hydrocarbon Receptor Nuclear Translocator (ARNT) Period/ARNT/Single-Minded (PAS)-B Mutants. After expression, cell pellets were harvested, resuspended in 20 mL of 50 mM Tris (pH 7.5), 17 mM NaCl, and 20 mM imidazole, lysed by high-pressure extrusion, centrifuged, and filtered (0.45-μm pore size). The supernatant was then injected over a Ni^{2+}–nitrilotriacetic acid (NTA) affinity column and eluted by using a linear 20–500 mM imidazole gradient. His_6-tagged ARNT PAS-B mutants eluted from the column were exchanged into an imidazole-free buffer, and followed by His_6 tag cleavage overnight using His_6-tobacco etch virus (TEV) protease. Another pass over a Ni^{2+}-NTA column was used to remove His_6-TEV and free the His_6 tag, and the remaining protein was concentrated in an Amicon pressure-driven ultrafiltration cell with YM10 10-kDa filters. The molecular mass of the purified protein, which contains a 4-residue vector-derived N-terminal cloning artifact (GAMD) followed by residues 351–470 of human ARNT, was confirmed for the wild-type protein by electrospray ionization mass spectrometry and for the mutants by DNA sequencing.

Equilibrium Denaturation/Renaturation Measurements. All experiments were carried out at 25 °C in 50 mM sodium phosphate (pH 7.5), 17 mM NaCl. Guanidine hydrochloride (Gdn·HCl)-induced equilibrium denaturation/renaturation experiments were performed after 24 h of equilibrating protein samples in buffers containing different concentrations of denaturant. Equilibrium measurements were monitored by using a Fluorolog-3 spectrofluorometer (JY Horiba). Intrinsic tryptophan fluorescence emission spectra were recorded between 290 and 380 nm with excitation at 295 nm in a 4-mm pathlength cell. Best-fit curves were generated by using nonlinear regression, and the locations of maximum emission intensity were identified by calculating the first derivative of these spectra and finding the position where the first derivative is zero.

Deuterium Exchange. Initially, ^{15}N-labeled ARNT PAS-B samples [in 50 mM Tris (pH 7.5), 17 mM NaCl] were lyophilized and resuspended in 99% D_2O, starting the deuterium exchange reactions. ^{15}N-^{1}H HSQC spectra were sequentially recorded every 20 min. Afterward, the pH was recorded, and deuterium exchange rates were calculated by using NMRView (1), converting these into protection factors by using the approach of Bai *et al.* (2).

To confirm that these measurements were made under EX2 conditions, we examined the pH dependence of the ^{2}H exchange rates for wild-type ARNT PAS-B. As expected, we observed a significant decrease in these rates at lower pH. Comparing the exchange rates at pH 6.76 and 7.63 (uncorrected, measured pH after exchange), we found an average ratio of exchange rates of 0.163 [k_{ex} (pH 6.76)/k_{ex}(pH 7.63)] for $n = 19$ sites. This compares favorably with a calculated ratio of 0.135 given these pH values, confirming EX2 conditions.

1. Johnson BA, Blevins RA (1994) NMRView: A computer program for the visualization and analysis of NMR data. *J Biomol NMR* 4:603–614.
2. Bai Y, Milne JS, Mayne L, Englander SW (1993) Primary structure effects on peptide group hydrogen exchange. *Proteins* 17:75–86.
3. Card PB, Erbel PJ, Gardner KH (2005) Structural basis of ARNT PAS-B dimerization: Use of a common β-sheet interface for hetero- and homodimerization. *J Mol Biol* 353:664–677.

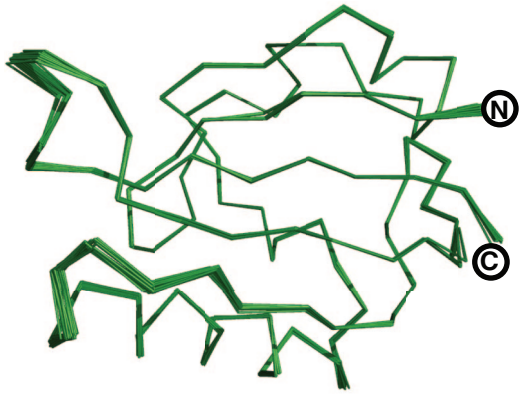

Fig. S1. Solution structure of ARNT PAS-B F444Q/F446A/Y456T. Superposition of 20 lowest energy backbone structures of ARNT PAS-B mutant in conformation **2** (residues 361–461, flexible termini not shown).

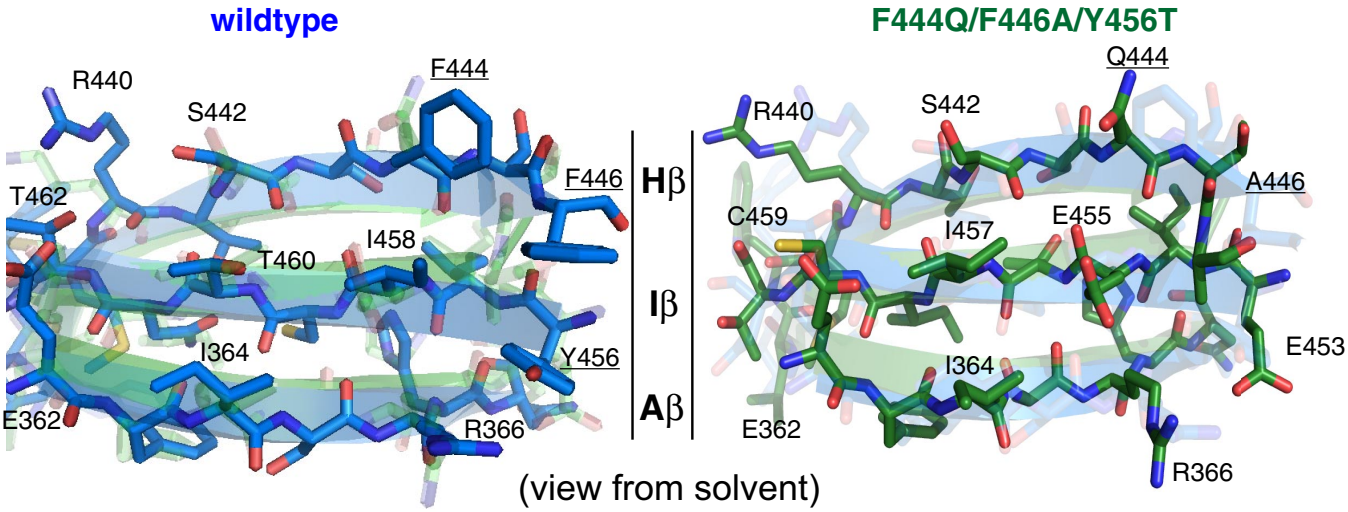

Fig. S2. Residues adopt a similar conformation in both structures. Solvent-exposed residues on the β-sheet surface of both wild-type and mutant conformations adopt similar conformations but display different chemical groups leading to significant differences in binding affinity for ARNT targets.

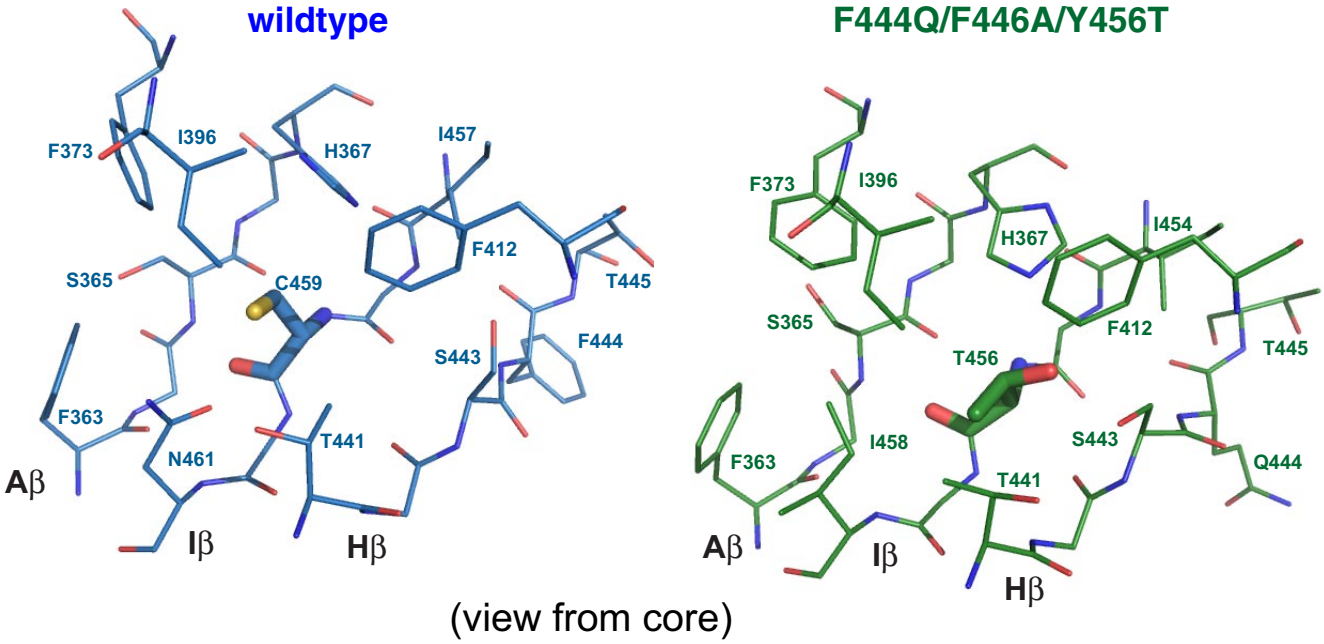

Fig. S3. Core residues adopt a similar conformation in both structures. Buried residues within 5 Å of C459 (conformation **1**) or T456 (conformation **2**) adopt similar conformations. Note that residue 444 is the only solvent-exposed side chain shown.

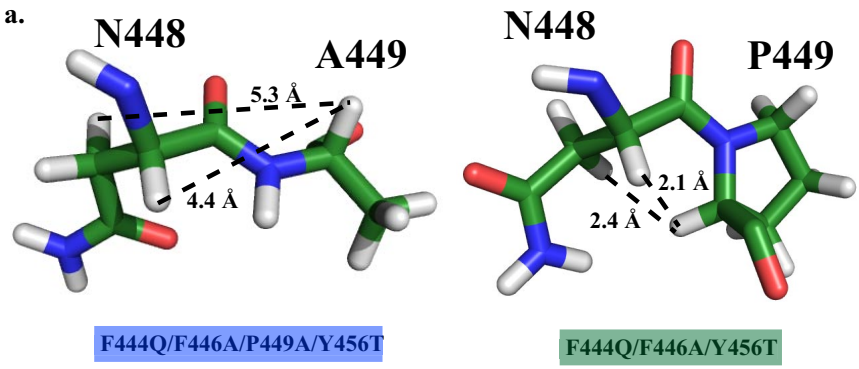

b.

Atom Number	F444Q/F446A/P449A/Y456T (ppm)	F444Q/F446A/Y456T (ppm)
N448.HA	4.439	4.436
N448.HB1	2.788	2.684
N448.HB2	2.788	2.663
A449.HA	4.083	-
P449.HA	-	4.566

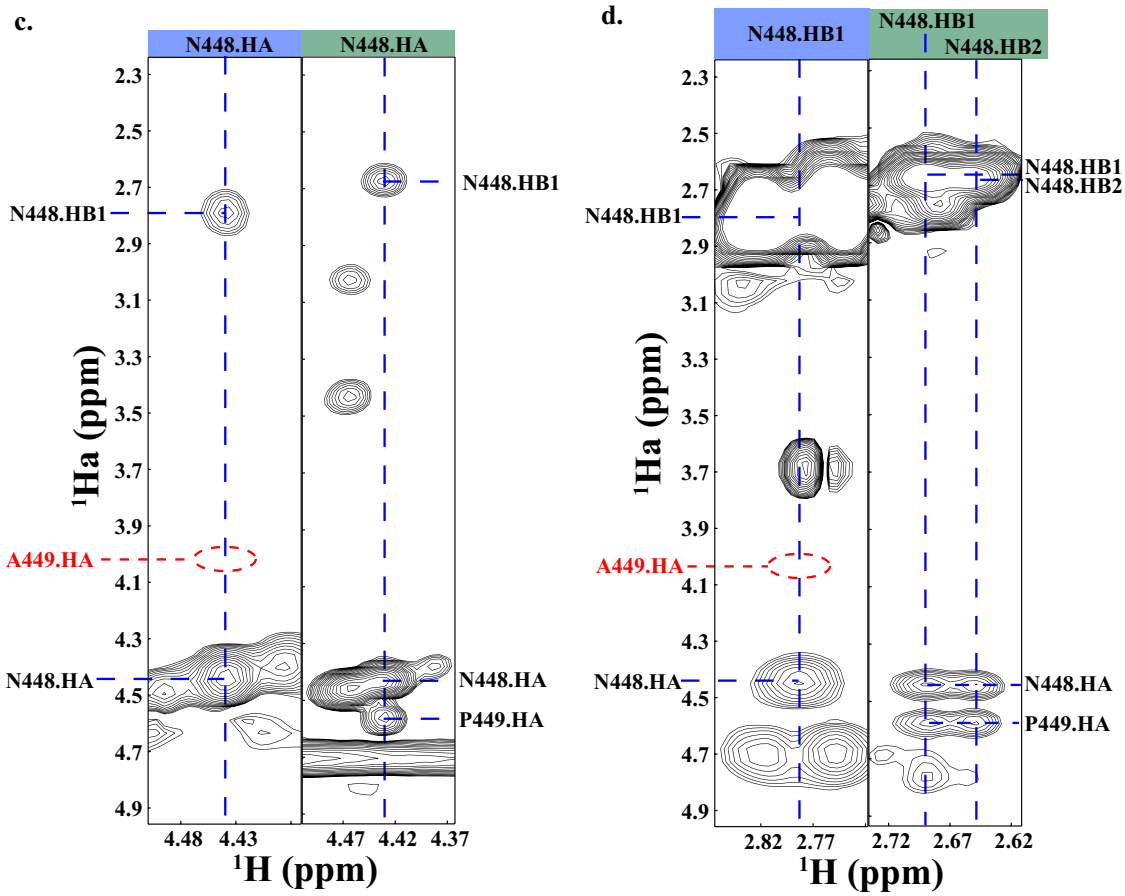

Fig. S4. NOE data establishing the configuration of the 448–449 peptide bond in F444Q/F446A/Y456T and F444Q/P449A/F446A/Y456T ARNT PAS-B. (*a*) Measured distances between N448 HA/HB* and A449 HA or P449 HA in models for *trans* and *cis* configurations in the N448/P449A or N448/P449 peptide bond. The *trans* model, corresponding to F444Q/F446A/P449A/Y456T, was generated from the ARNT PAS-B wild-type structure (3), replacing the P449 side chain with an alanine. The *cis* model is from the solution structure of F444Q/F446A/Y456T, reported here. (*b*) ^{1}H chemical shift assignments for N448, P449, and A449. (*c*) Observed NOEs involving N448 HA or HB* for both mutants. The presence of a strong α_i/α_{i+1} cross-peak between N448 and P449 confirms the *cis* conformation for F444Q/F446A/Y456T, whereas the absence of the corresponding cross-peak between N448 and A449 in F444Q/F446A/P449A/Y456T supports a *trans* configuration. (*d*) β_i/α_{i+1} cross-peaks between N448 and P449 (or A449) also support these assignments.

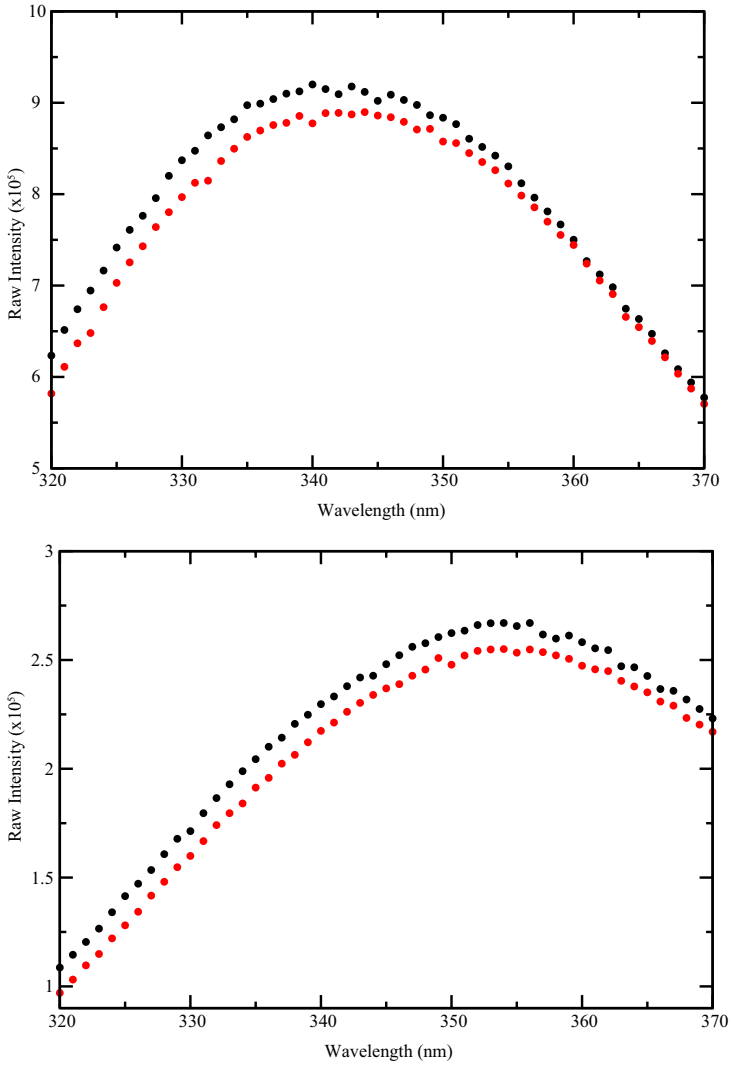

Fig. S5. Two tryptophan residues within ARNT PAS-B have similar local environments throughout the unfolding process in both conformations. Tryptophan fluorescence emission spectra reveal a similar local environment for the 2 ARNT PAS-B tryptophan residues for the wild-type (black circles) and F444Q/F446A/Y456T (red circles) proteins under both native (*Upper*) and denaturing conditions (3 M Gdn·HCl; *Lower*).

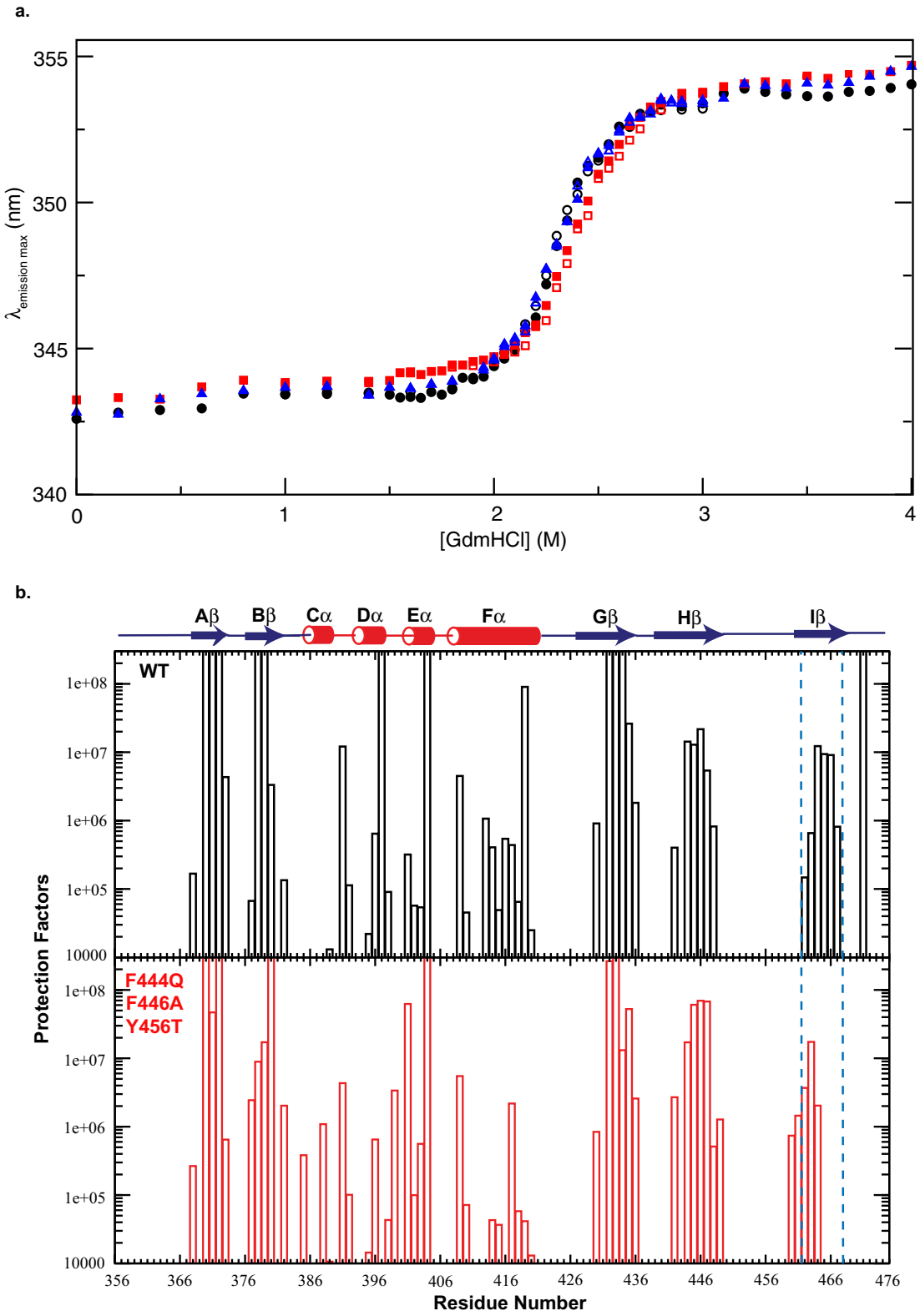

Fig. S6. ARNT PAS-B mutants have global stabilities similar to those of wild type. (*a*) Equilibrium denaturation behavior of ARNT PAS-B wild type (black circles), Y456T (blue triangles), and F444Q/F446A/Y456T (red squares), monitored by shifts in the wavelength maximal intensity in tryptophan fluorescence emission spectra. Gdn·HCl denaturation is reversible as shown by the similarity of denaturation (filled symbols) and renaturation (open symbols) profiles. (*b*) ^{2}H exchange protection factors of wild type and F444Q/F446A/Y456T ARNT PAS-B.

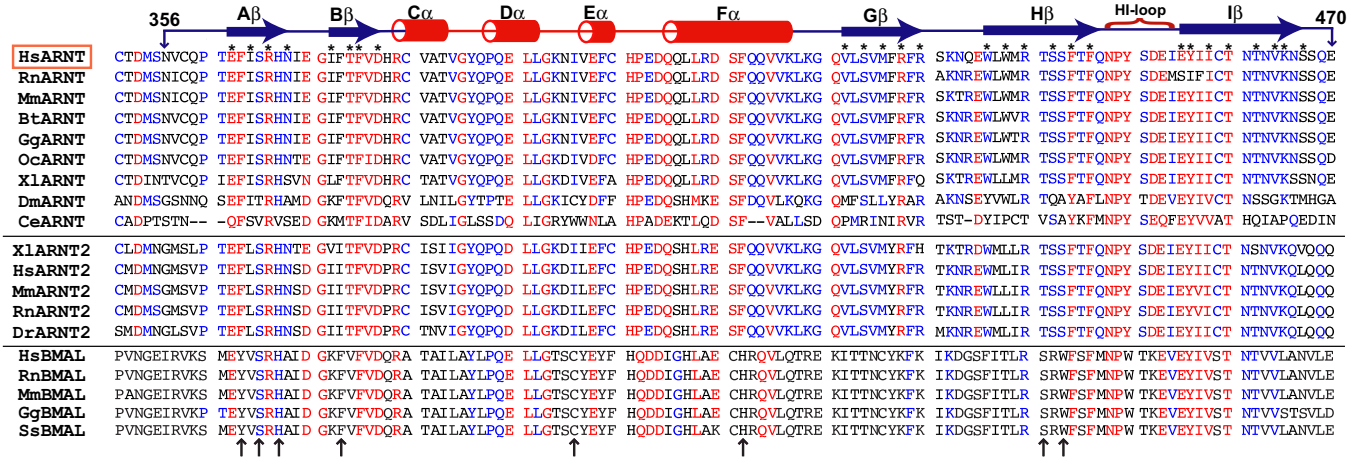

Fig. S7. Multiple sequence alignment of human ARNT, several homologs, and brain and muscle ARNT-like (BMAL) homologs. Human ARNT and its homologs align well throughout most of the domain, whereas BMAL shows poor sequence alignment. (*, solvent-exposed residues for ARNT PAS-B wild-type β-strands; ↑, residues within 5 Å of C459 (conformation **1**) or T456 (conformation **2**).

Table S1. Statistics for ARNT PAS-B F444Q/F446A/Y456T solution structure determination

Structural analysis	
NOE distance restraints	
Unambiguous	2,688
Ambiguous	490
Hydrogen bond restraints	50
Dihedral angle restraints	133
Mean rmsd from experimental restraints	
NOE, Å	0.033 ± 0.001
Dihedral angles, °	0.0044 ± 0.0321
Average no. of	
NOE violations >0.5 Å	0
NOE violations >0.3 Å	0.45 ± 0.50
Dihedral violations >5°	0
Mean rmsd from idealized covalent geometry	
Bond lengths, Å	0.0039
Bond angles, °	0.54
Impropers, °	0.47
Geometric analysis of residues 360–462	
rmsd from the mean	
Backbone atoms, Å	0.28 ± 0.08
All heavy atoms, Å	0.68 ± 0.07
Ramachandran analysis (PROCHECK)	
Most-favored region, %	71.8
Additionally allowed region, %	24.5
Generously allowed region, %	2.7
Disfavored region, %	0.8